MATCH
Communications in Mathematical and in Computer Chemistry

MATCH Commun. Math. Comput. Chem. **81** (2019) 557-578

ISSN 0340 - 6253

Chemical Reaction Networks Associated with the Hilbert's 16^{th} Problem. Limit Cycles and Stability Analysis

Gefry Barad*, Eugen Czeizler, Andrei Păun

National Institute of Research and Development for Biological Sciences, Department of Bioinformatics, Bucharest, Romania

gbarad@gmail.com; gefry.barad@incdsb.ro, eugen.czeizler@incdsb.ro, andreipaun@gmail.com

(Received July 13, 2018)

Abstract

We give examples of 2-parameter bounded quadratic dynamical systems with 3 finite singularities, which have at least 4 limit cycles around a singularity (in the (4,0)-configuration) - the first example of this type - and in a (3,1)-configuration. The paper mentions the Nanobiotechnological origins of these experimentally discovered systems with interesting properties.

1 Introduction. Chemical Reaction Networks. Topics approached using CRN's and dynamical systems

We consider the following Chemical Reaction Network (CRN) with 4 species, A, B, C and 0, given by the reversible reactions (MAK): $A+B \to C$, $\quad B+C \to A$, $\quad C+A \to B$ $A+A \to 0$, $\quad B+B \to 0$, $\quad C+C \to 0$. Some kinetic rates could be zero. A particular case of this CRN is given by $A+B \to C$, $B+C \to A$, $C+A \to B$. In [1], it was studied as a programming problem of 1-dimensional staged assembly, and also as an optimization problem solved in Copasi software: find the initial concentrations of A, B and C and the

distribution of time and concentrations required by 5 stages of this CRN, to get maximum yield of A.

Suggested by nano-biotechnological applications, in [2] Demaine et al. introduced an enhanced version of the abstract TAM of Wang tiles. and later, using 1-dim-HAM , the above Chemical Reaction Network (CRN) was programmed in RuleBender software by an INCDSB team [3], [4]. A possible rule – based modeling of this CRN is the following: A:= the set of 1-dimensional oriented linear strings made on the alphabet $\{a, b, c\}$, which ends and begin with b and c (or vice-versa). Analogous definitions for B and C. The strings can glue themselves or be broken with probabilities based on the number of elementary letters, the length of the linear assembly, the glue function between 2 letters. We are interested in the concentration of length n strings in time.

Our simulations [3] show an oscillatory behavior of string concentrations for some special values of n; the rest of the other length values being of very small concentrations. These results are contrary to some intuition for the following reasons. Given a stable molecular concentration of A in the CRN above, any tile-molecule of A is a result of a specific staged assembly using a binary tree of directional chemical reactions; simulations show that some paths are more probable than the other. Also, a deep theorem of [5] reformulates the Four Color Theorem (for which there is no computer-independent proof) in terms of non-associative calculus in the quaternionic algebra (vector-cross product of i, j, k) and a model is the initial chemical reaction above: we also have 0 as a 4^{th} species.

Copasi and BioNetgen simulations are not chemically relevant for negative concentrations, so the choice was a Mathematica environment. Stochastic (NFSim), deterministic and rule-based modeling oscillatory behaviors are different, as mentioned in [6]. A classical CRN approach: stoichiometry, persistence, thermodynamic rules and Lyapunov functions, Deficiency Zero/One Theorems – does not explain this oscillatory behavior.

In a canonical way we can associate to any CRN a dynamical system of species concentrations. In our case, if we impose that the concentrations of A, B and C are equal, we get a 2-dimensional polynomial dynamical system of type: $\frac{dx}{dt} = qy^2 - rx$, $\frac{dy}{dt} = py^2 + sx - mxy + ny$. The backward road is not always possible: to find a CRN with a given dynamics. The following chemical reaction network: $Y() \to Y() + Y()$ (kinetic rate $k_1 = 0.2$) ;$X() + Y() \to X() + P()$ ($k_2 = \frac{2}{3}$); $Y() + Y() \to X() + Y()$ ($k_3 = \frac{6}{10}$); $S() + X() \to Y() + Y()$ ($k_4 = \frac{1}{3000000}$); $X() \to P()$ ($k_5 = \frac{2}{3}$) has the associated dynamical

system:

$\frac{dx}{dt} = -x + 0.6y^2$; $\frac{dy}{dt} = -0.6y^2 + \frac{2}{3}x - \frac{2}{3}xy + 0.2y$; x and y are the concentrations of X and Y from the CRN above. The concentrations of S and P are constant and high. This system is linearly equivalent to the dynamical system (3) for $p = 0$ and $B = 0.6$.

To study the experimentally observed limit cycles of this dynamical system, we have to insert it into a family of planar quadratic systems. Few examples of stability analysis of this type of dynamical systems were performed by Perko, Roussarie, Rousseau, Llibre and Zhang [7] [8] [9] [10]. Our mathematical results are important for the Hilbert's 16^{th} problem.

2 The Hilbert's 16^{th} problem. Planar bounded quadratic dynamical systems

The maximum number and the position of the limit cycles for a planar quadratic system

$$\begin{array}{l} \dot{x} = a_1 + b_1 x + c_1 y + d_1 x^2 + e_1 xy + f_1 y^2 \\ \dot{y} = a_2 + b_2 x + c_2 y + d_2 x^2 + e_2 xy + f_2 y^2 \end{array} \tag{1}$$

(The Hilbert's 16^{th} problem (1900, Paris) in dimension 2) is still open [11]. If for every initial condition (x_0, y_0), the set $\{(x((x_0,y_0),t), y((x_0,y_0),t)) \mid t \geq 0, (x(t), y(t)) \text{ solution for}(1)\}$ is bounded in the plane, then using affine transformations and time parametrizations, the system (1) can be brought to the form [12]:

$$\left\{ \begin{array}{l} \dot{x} = -x + \beta y + y^2 \\ \dot{y} = \alpha x - (\alpha\beta + \gamma^2) y - xy + c(-x + \beta y + y^2), \end{array} \right. \tag{2}$$

$c \in (-2, 2)$, $\alpha > \beta + 2\gamma$ and $\gamma > 0$

These systems were studied by Perko, Dumortier, Roussarie [12], Llibre [8], Koditschek, Narendra and Dickson [13]. Perko conjectured in [12] that any bounded quadratic system has at most 2 limit cycles. For the full Hilbert's problem it is conjectured that the systems (1) have at most 4 limit cycles. Bounded quadratic dynamical systems are ubiquitous in Biology and Chemistry [14], [15].

Examples of quadratic systems with 4 limit cycles are given by Shi [16], Wang and Chen [17], Perko, Rousseau and Schlomiuk [18], Kuznetzov and Leonov [7] and others. There are standard numerical procedures [7] to localize stable limit cycles; also, it is almost impossible to vizualize "*small*" limit cycles, resulted from the coefficient perturbations [7].

The problem to find planar quadratic systems with 4 limit cycles in (0,4)-configuration was stated in [19].

We consider the following system which depends on 2 parameters B and p

$$\begin{cases} \dot{x} = -x - 0,8y + 0,4y^2 \\ \dot{y} = \left(2 - \frac{p}{0,4}\right) x + (1-2p)y - xy - (B-p)y^2. \end{cases} \tag{3}$$

It is a bounded quadratic system: for $x = u$ and $y = \frac{v}{\sqrt{0.4}}$,

$$\begin{cases} \dot{u} = -u - 2\sqrt{0.4}v + v^2, \\ \dot{v} = \left(2\sqrt{0.4} - \frac{p}{\sqrt{0,4}}\right) u + (1-2p)v - uv - \frac{B-p}{\sqrt{0.4}}v^2 \end{cases} \Rightarrow$$

$\Rightarrow \beta = -2\sqrt{0.4},\ c = \frac{p-B}{\sqrt{0.4}},\quad \alpha = c + 2\sqrt{0.4} - \frac{p}{\sqrt{0.4}} = 2\sqrt{0.4} - \frac{B}{\sqrt{0.4}};\ \gamma = \sqrt{0.6}.$
We draw the bifurcation diagram of the 2-dimensional (B,p)-family in the (α, c)-coordinate system. $(\alpha, \beta, \gamma, c)$ is the 4-uple which characterize any bounded quadratic system $-2 < c < 2$ and $\alpha > \beta + 2\gamma$.

The range of the parameters B and p is defined as the range of $(\alpha, \beta, \gamma, c) = (\alpha, -2\sqrt{0.4}, \sqrt{0.6}, c)$ such that the dynamical systems (3) are bounded, with 3 singularities.

We numerically detected limit cycles for certain values of B and p. We are interested to mathematically prove the existence of these limit cycles. The problem of proving the existence of computer-detected limit cycles was recently studied by Giacomini and Grau [20], [21], [22].

The local stability analysis for (3) as bounded quadratic systems is made following [12], [9], [10]. The hand calculations are followed by the computer – assisted ones for the Lyapunov values and for the real parts of the Poincaré normal form coefficients. For $p = 0$ and $B = 0.5 * \left(1.7 - \sqrt{1.29}\right)$ there is a Hopf bifurcation of codimension 2. The construction of the Poincaré-Bendixson regions are based on the normal form [18] for the small cycles, and on a technical lemma of Gasull, Grau, Giacomini [22] for the normal size ones. We apply this lemma in our case, where we use a kind of coordinate system based on the Catalan's trisectrix – also known as L'Hospital's cubic or the Tschirnhausen Cubic.

3 Results

- A family of bounded quadratic dynamical systems which depends on 2 parameters, with 3 finite singularities, which have at least 4 limit cycles around a singularity is

presented. It is the first example of this type of (4,0)-configuration. By definition, an (i, j)-configuration means that one singular point is surrounded by i limit cycles and a second one is surrounded by j limit cycles.

- The existence of two "*new*" normal size limit cycles (numerically detected in Perko's terminology) is proved using topological insight into the local bifurcation diagram of the family of dynamical systems. We apply the well established results from the local theory of planar quadratic systems in the case of the systems (3), and new numerical results from Section 5.

- Some members of the family represent the dynamics of species concentrations of a chemical reaction network (CRN), able to be specifically analyzed with dedicated software.

4 Theory and computations. The local Stability analysis. Bifurcations

4.1 The 1-dimensional Hopf bifurcations

For fixed B, the systems (3) form a (mod dx) family of rotated vector fields [23]. In particular they have the same fixed points (singularities) for any fixed B and variable p (as for $p = 0$).

$$\begin{aligned} \dot{x} &= -x - 0.8y + 0.4y^2 \\ \dot{y} &= 2x + y - xy - By^2 + \tfrac{p}{0.4}\left(-x - 0.8y + 0.4y^2\right). \end{aligned} \tag{4}$$

The computations of the 3 singular points (x_i, y_i) : $x = 0.4y^2 - 0.8y$ *and* $0.8y^2 - 1.6y + y -$

$$-y\left(0.4y^2 - 0.8y\right) - By^2$$

$$= -0.4y^3 - 0.6y + (1.6 - B)y^2 = 0. \tag{5}$$

$y_0 = x_0 = 0$ and y_1 and y_2 are solutions of $0.4y^2 - (1.6 - B)y + 0.6 = 0$,

$\Delta > 0 \Leftrightarrow (1.6 - B)^2 > 0.96 \Leftrightarrow |1.6 - B| > \sqrt{0.96}$,

$B = -c\sqrt{0.4} \in \left(-\sqrt{1.6}, \sqrt{1.6}\right) \Rightarrow B < 1.6 - \sqrt{0.96} \approx 0.62$ and $B > -\sqrt{1.6}$.

$y_1 = \frac{1.6 - B - \sqrt{(1.6-B)^2 - 0.96}}{0.8}$ and $x_1 = 0.4y_1^2 - 0.8y_1$; $\quad (x_1, y_1)$ is a saddle

$y_2 = \frac{1.6 - B + \sqrt{(1.6-B)^2 - 0.96}}{0.8}$ and $x_2 = 0.4y_2^2 - 0.8y_2$; $\quad (x_2, y_2)$ is a stable node (or focus).

$B \in \left(-\sqrt{1.6}; 1.6-\sqrt{0.96}\right)$. For $B = 1.6-\sqrt{0.96}$ we have a system with 2 fixed points for any p, and a saddle-node bifurcation.

The Jacobian of the system (3) is $\begin{pmatrix} -1 & -0.8+0.8y \\ 2-\frac{p}{0.4} & 1-2p-x-(2B-2p)y \end{pmatrix}$. The Jacobian computed in the origin: $J(0) = \begin{pmatrix} -1 & -0.8 \\ 2-\frac{p}{0.4} & 1-2p \end{pmatrix}$, the characteristic equation is $z^2+2pz+0.6=0$, $z_{1.2} = -p \pm i\sqrt{0.6-p^2}$ if $|p| < \sqrt{0.6}$. $\frac{\partial Re(z_c)}{\partial p} \neq 0 \Rightarrow$ we have a 1-dim Hopf bifurcation for $p=0$.

The stability of the origin and the type of the Hopf bifurcation is given by the first Lyapunov value σ for $p=0$ [9], which is computed as follows:

$\dot{x} = ax+by+p(x,y), \qquad \Delta = ad-bc > 0, a+d=0, p = \sum_{i+j=2} a_{ij}x^iy^j, q = \sum_{i+j=2} b_{ij}x^iy^j.$

$\dot{y} = cx+dy+q(x,y).$ In the case of our dynamical systems (3): $a_{20} = a_{11} = b_{20} = 0$

$\sigma = \left(\frac{-3\pi}{2b\Delta^{\frac{3}{2}}}\right)\left(aca_{02}b_{11} + abb_{11}^2 + 2c^2a_{01}b_{02} - 2acb_{02}^2 + (bc-2a^2)\,b_{11}b_{02}\right) =$

$\frac{-3\pi}{2b\Delta^{\frac{3}{2}}}\left(1.6-3.2B+4B^2-3.6B\right) = \left(B^2-1.7B+0.4\right)e,\ e>0,\ B_{1,2} = \frac{1.7\pm\sqrt{1.29}}{2}.$ $B_1 = B_- = \frac{1.7-\sqrt{1.29}}{2}$.

For $B \in \left(B_-, 1.6-\sqrt{0.96}\right)$ the origin is stable and the Hopf bifurcation is supercritical. For $B \in \left(-\sqrt{1.6}, B_-\right)$ the origin is unstable and the Hopf bifurcation is subcritical.

For $B = B_- = \frac{1.7-\sqrt{1.29}}{2}$ the origin is a weak focus of order 2 ($\sigma = 0$). It is unstable because the second Lyapunov value, $W_2 > 0$. Its sign of is computed symbolically using the formulae from [18] and [24]. For a planar quadratic dynamical systems as below:

$$\begin{cases} \dot{x} = -y + ax^2 + bxy + y^2 \\ \dot{y} = x + cx^2 + dxy. \end{cases} \tag{6}$$

$$Sign\ of\ W_2 = sign\left(-5cd^3+9acd^2+5cd^2-abd^2-bd^2-20c^3d-19bc^2d+\right.$$

$$+b^2cd+18a^2cd+8acd+10cd-a^2bd+18abd+19bd-40ac^3-18abc^2-10bc^2-$$

$$\left.-9ab^2c-5b^2c-40a^3c-40a^2c+20ac+5ab^3+5b^3+20a^3b+40a^2b+40ab+20b\right).$$

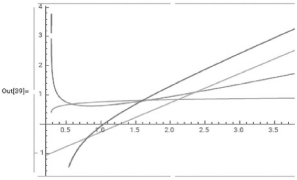

Figure 1. Bifurcation diagram; the number of limit cycles is locally constant in connected 2-dim and 1-dim domains

We explain the local bifurcation diagram for the dynamical systems (3). For each pair (B,p), we define the pair (α, c): $\alpha = \sqrt{1.6} - \frac{B}{\sqrt{0.4}}$, $c = \frac{p-B}{\sqrt{0.4}}$; we can recover the coefficients B and p. $\beta = -\sqrt{1.6}$ and $\gamma = \sqrt{0.6}$ are fixed. Each system from the family (3) represents a point in the bifurcation diagram.

Ox-axis= the range of the α coefficients and Oy -axis= the range of the c -coefficients.

The parabolic curve, asympotic to the oy-axis, is the Hopf bifurcation curve for the second anti-saddle (x_2, y_2).

1 dim-Hopf bifurcation curve around the origin (the line) has the equation:

$c = \alpha + \frac{1+\gamma^2}{\beta}$ = the relation between c and α coefficient such that the trace of the Jacobian in the origin is zero.

Saddle-saddle connection (the upside-down parabolic curve) has the equation

$c = \frac{1}{2}\left(\alpha + \beta + \sqrt{(\alpha-\beta)^2 - 4\gamma^2}\right)$ = the relation between c and α coefficient such that there is a saddle-saddle connection between the saddle (x_1, y_1) and the point $[0; 0; 1]$ from the Poincaré sphere (the structure of Figure 4, Type II for the stable manifolds).

Perko [9] proved the existence of the local homoclinic loop bifurcation curve and of the local multiplicity 2 limit cycles bifurcation curve. Figure 1 is completed by Figure 3, where there is the multiplicity 2 limit cycle bifurcation curve, tangent to the Hopf bifurcation curve for the value $B = B_- = (1.7 - \sqrt{1.29})/2$. The most complete bifurcation diagram is Figure 7, where there is the number of local and non-local limit cycles around the weak focus of order 2.

4.2 The 2-dimensional Hopf bifurcation

It is proved in [12] the existence of the multiplicity – 2 limit cycle $surface$, which is given for fixed γ, in the (α, c, β)-coordinates as the graph of an analytical function. Fixing β will provide a curve in the (α, c)-plane = P, which is tangent to the Hopf bifurcation line (Chow's Theorem) for the value $B = B_- = (1.7 - \sqrt{1.29})/2$ and p=0. We identify the position of this curve in the plane P. The intersections between P and the 1-dim Hopf bifurcation surface (which is the line $c = \alpha + \frac{1+\gamma^2}{\beta}$), and also to the multiplicity 2 – limit cycle bifurcation surface are transversal and they look like Figure 3. More exactly, for the dynamical systems (3), the local zone from the bifurcation diagram containing 2 limit cycles is located below the line– 1-dim Hopf curve from Figure 1 (or the line from Figure 7) for negative p, in the supercritical Hopf bifurcation zone, for

$B \in \left(B_- = \frac{1.7-\sqrt{1.29}}{2}, 1.6 - \sqrt{0.96}\right)$. It is the generic topological picture when the origin is unstable ($W_2 > 0$). The dynamical systems (3) have two limit cycles around the origin (small, local limit cycles resulted from coefficient perturbations) if the signs of the coefficients of equation (7) below alternate, as a necessary condition according to [18].

We apply Rousseau-Schlomiuk Theory [18] (Theorem 2.11) to determine the position of the multiplicity 2-bifurcation curve in the (B, p) plane: in polar coordinates which came from the Poincaré normal form, around the weak focus of order 2 for the system with $p = 0$ and $B = B_-$, the number of the limit cycles is the number of strictly positive roots of the equation:

$$Re\,(c_0) + Re\,(c_1)\,r + Re\,(c_2)\,r^2 = 0, \quad Re\,(c_0) = \lambda. \tag{7}$$

The system (3) has to be brought to the form of the dynamical system (8) using affine transformations and time parametrization. The coefficients of the eq. (7) are computed using the the coefficients of:

$$\begin{cases} \dot{x} = \lambda x - y + ax^2 + bxy + y^2 \\ \dot{y} = x + \lambda y + cx^2 + dxy \end{cases} \tag{8}$$

$Re\,(c_1) = \frac{1}{8}(b(a+1) - c(d+2a))$ and $Re\,(c_2) = \frac{1}{288}W_2$. The formula for W_2 followed the equation (6). Using the linear transformation:
$\begin{pmatrix} u \\ v \end{pmatrix} = \begin{pmatrix} e & f \\ g & h \end{pmatrix} \begin{pmatrix} x \\ y \end{pmatrix}$, where $e = \frac{-(p^2-pB+B)+\sqrt{(p^2-pB+B)^2+1.6(1+p-2B)(1-p)}}{0.8(1+p-2B)}$,
$f = 1$, $g = (B-p)e - 1$, $h = 0.4e$, then scaling (diagonal transformation) and linear time parametrization, we bring the dynamical system (3) to the form of the system (8) [18]. Using Mathematica, we compute the discriminant of the equation (7) and the local number of limit cycles appears. The implicit analytical formula for the multiplicity 2 – limit cycle curve is given by the discriminant of the equation (7) when it vanishes.

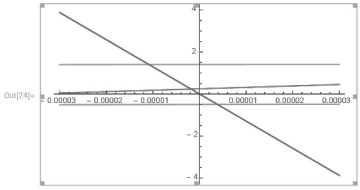

Figure 2. Mathematica computations: The line with negative slope:= the trace. The almost horizontal lines are: the second focal value, the discriminant of the equation (7) and the first focal value (the lowest line)

Remark. The Normal Form Theory provide the universal unfolding for the codim 2 bifurcation at a weak focus of order 2 ([12] and Theorem 6, Chapter 4.15 from [9]): if the system has a weak focus of order 2 (the trace and the first Lyapunov values are zero), there is a change of variables such that there is a family of bounded quadratic systems whose coefficients depend on 2 parameters, whose bifurcation diagram is given by the Figure 3:

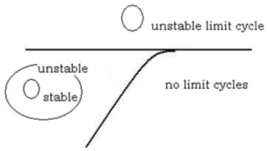

Figure 3. The local bifurcation diagram around a weak focus of order 2.

Unfortunately, this local chart around the weak focus of order 2 is not in the (α, c)-plane $= P$. The above mentioned theorems from [12] and [18] are required to complete the picture. Mathematica implementations double-checked the zones of different signs for the coefficients of the equation (7) and help us to properly attach Figure 3 to the local bifurcation diagram of Figure 1, as described in the beginning of the Section 3.2. We had four possibilities to attach Figure 3, *or* its mirror image, from the time reversal situation, to the tangency point (the 2-weak focus).

For fixed β and γ of the system (2), the weak focus of order 2 is the solution of the system

$$c = \alpha + \frac{1+\gamma^2}{\beta} = \frac{\alpha\beta - 2\alpha^2 - 1 + \sqrt{(\alpha\beta - 2\alpha^2 - 1)^2 - 4(\alpha - \beta)(\beta - 2\alpha)}}{2(\beta - 2\alpha)}.$$

It is a degree 3 equation in α. For $\frac{1+\gamma^2}{\beta} = \beta$ the equation become of degree 2, $\alpha = \alpha(\beta, \gamma)$ is the only solution such that $\alpha > \beta + 2\gamma$ and $c \in (-2, 2)$.

Remark. There are two instances where we use $\beta < 0 < \gamma$ and the imposed relation $\frac{1+\gamma^2}{\beta} = \beta$ between β and γ. The first situation is motivated by the hand-calculations from Section **2.2** which confirm that the Figure 3 is also the bifurcation diagram around the weak focus of order 2 in the (α, c) -plane, attached as described at the beginning of this section. The second situation where we use this relation and $\beta = -\sqrt{1,6}$ is required by numerical simulations from Section **5**.

5 Separatrix configurations

It is known the phase portrait for a bounded quadratic system with 3 singularities (the topological structure of the stable and the unstable monifolds of the saddle, without the exact number of limit cycles) [12], [9], [25]. From these seminal works we record that for our systems (3) we have the following topological possibilities.

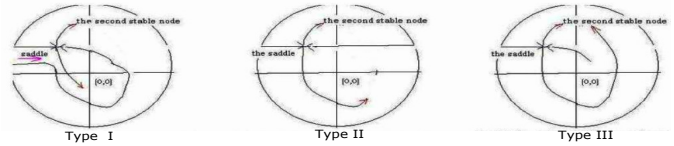

Figure 4. The three possible topological structures for the unstable and stable manifolds of the saddle
Type I: both stable manifolds came from "*the left infinity*" to the saddle
Type II: there is a saddle-saddle connection between the finite saddle and the point $[0, 0, 1]$ from Poincaré sphere
Type III: both unstable manifolds converge to the second anti-saddle (or to a limit cycle which surround it)

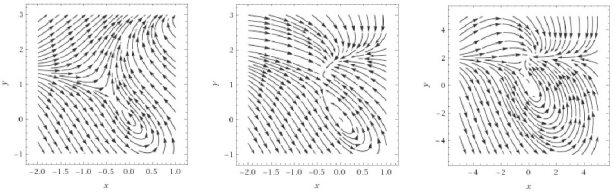

Figure 5. $p = 0$ and $B = 0.2$ The south separatrix from the saddle $(-0.3; 0.5)$ converges to the second anti-saddle (Type III). $p = 0$ and $B = 0.61$. The east separatrix (stable manifold) came from left infinity towards the saddle (Type I). $p = 0$ and $B = \frac{3}{\sqrt{40}}$. There is a saddle-saddle connection between the saddle and the $[0, 0, 1]$ from Poincaré sphere (Type II)

6 New (non-local) limit cycles around the origin

For $B = 0.2$ and $p = 0$ the origin is unstable (the first Lyapunov value > 0) and locally the field lines spiral out. We numerically detect that the Poincaré map, the cross-section map with respect to Oy, satisfies $P(z) < z$ for the initial conditions $x = 0$, $y = 0.001$. So,

we have a stable limit cycle. For the initial conditions $x = 0$, $y = 0.05$, $P(z) > z$, so we have a bigger unstable limit cycle.

The consequences of this enriched diagram are:

1) the existence of 4 limit cycles in $(4, 0)$- configuration in the "2-limit cycle" local zone. This is a new fact that answers a question from [19] on the maximum number of limit cycles around a singularity for a planar quadratic dynamical system.

2) the existence of 4 limit cycles around the $(0, 0)$ and (x_2, y_2) in $(3, 1)$-configuration: around the origin we have the 2 numerically detected limit cycles above and a 3^{rd} one from the subcritical Hopf bifurcation for $p > 0$. For $B_3 = \frac{-1-\sqrt{6}}{5}$, $Tr\left(J_{(x_2,y_2)}\right) = 0$. For positive p close to 0 and variable B close to B_3 we have a supercritical Hopf bifurcation for (x_2, y_2), giving birth to the 4^{th} limit cycle around (x_2, y_2).

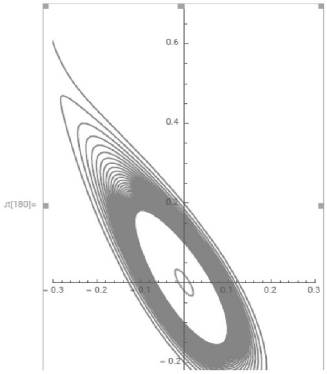

Figure 6. Poincaré map based on Oy axis. B=0.2, p=0. Initial conditions on the Oy-axis: 0.1 for the expanding trajectory, and 0.02 for the smallest inside trajectory. Between these values $P(z)$ has a fixed point i.e. an unstable limit cycle; there is also a stable limit cycle because the origin is unstable

THEOREM 6.1 *For $B = 0.2$ and $p = 0$, the dynamical system* (3) *has at least a stable limit cycle surrounded by a bigger unstable limit cycle around the origin.*

PROOF 6.2 *The systems* (3) *have the ability to not enter in general conditions of many theorems which could prove the existence of these 2 limit cycles as for Lienard, Ricatti, Abel, polar or normal form systems etc. The problem for the Brusselator and for the Van der Pol oscillator was numerically approached in [20], [22], [21]. For a given system, it*

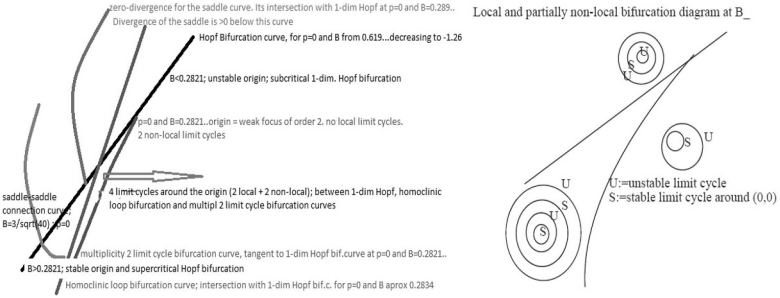

Figure 7. Enriched bifurcation diagram (local + non-local) around $(0, 0)$

was proved that the numerically detected cycle can be surrounded by a Poincaré-Bendixson zone defined by 2 trigonometric polynomials (i.e. its boundaries).

From [22] we will use Corollary 2.1 as follows: Let $C = Z(s) = (X(s), Y(s))$ *a parametrization of a smooth curve in* $\mathbb{R}^2$*. By definition,* C *is transversal to the flow given by the dynamical system* $(dx = P(x, y); dy = Q(x, y))$ *if* $F(s) = P(Z(s)) \cdot Y'(s) - Q(Z(s)) \cdot X'(s)$ *does not change sign and is zero at finitely many points called contact points.*

Corollary 2.1 from [22]: For a given open orbit segment of the dynamical system (1)*,* $\gamma(t)$ *and for any* ε *small enough we can find 4 curves,* ε*-close to* γ *(distance measured on the normal lines to* γ *at most* ε*), all transversal to the flow, inward or outward as desired, on different sides of* γ*.*

LEMMA 6.3 *The dynamical system* (3) *for* $B = 0.2$ *and* $p = 0$ *has a Figure 4 – Type III configuration of its stable and unstable manifolds: both unstable manifolds converge to the second anti-saddle (or to a limit cycle which surround it).*

PROOF 6.4 *Suppose that the separatrix configuration is given by Figure 4, type I. The origin is unstable and we automatically have an entrance zone for the flow, so we have a stable limit cycle. Inside it, for* $B > B_-$*, we have a small unstable limit cycle (from the local theory around the weak focus of order 2). Both have to disappear before the saddle-node bifurcation for* $B = 1.6 - \sqrt{0.96}$*. The stability of the homoclinic loop bifurcation is given by the sign of the divergence at the saddle* (x_1, y_1)*.* $Tr = Div\left(\frac{\partial f}{\partial x} + \frac{\partial g}{\partial y}\Big|_{(x_1,y_1)}\right) = \left(\frac{p}{0.4} - \frac{B}{0.8}\right)(0.8 - B - \sqrt{c}) + \sqrt{c} - 1$*, where* $c = (1.6 - B)^2 - 0.96$*. If the homoclinic loop bifurcation is not degenerate, the big stable limit cycle disappears first, then the small*

unstable one. But this is not possible: the positive divergence zone is below the curve $Div = 0$ *plotted in Figure 8.* $Div = 0$ *is the violet curve from Figure 7. For* $p = 0$*, on the Hopf bifurcation line,* $Div = 0$ *if* $B=(\sqrt{6}-1)/5$*=0.2898..., after the value of B for the order 2 weak focus: 0.282... in the supercritical Hopf bifurcation zone and before* $B = \frac{3}{\sqrt{40}}$*=0.474... where there is a saddle-saddle connection (Figure 4, Type II configuration: this B=0.474... is given by the intersection between the saddle-saddle connection curve and the Hopf bifurcation curve:* $p = 0$ ***and*** $c = \frac{1}{2}\left(\alpha+\beta+\sqrt{(\alpha-\beta)^2-4\gamma^2}\right)$*. Theorem 2.20 from [12] and [9]).*

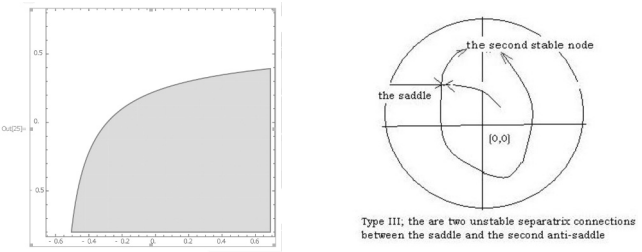

Figure 8. The curve p=f(-B) given by the divergence at the saddle = 0.

..

Next, we apply to our systems (3) *the following fundamental fact proved in [26]: Figure 4, Type I and III configurations alternate before and after a homoclinic loop bifurcation.*

We do not have a degenerate homoclinic bifurcation because of the saddle-saddle connection curve and its behavior under rotated vector fields [23] and [10]. Type II is almost a Type I – Figure 4 configuration of the unstable manifolds. Otherwise, after the degenerate degree 2 homoclinic bifurcation, increasing B from $(\sqrt{6}-1)/5$ *towards* $B = \frac{3}{\sqrt{40}} = 0.474..$*, another homoclinic bifurcation has to appear. So, for p=0 and B=0.2, as for any* $B \in \left(-\sqrt{1.6}, B_-\right)$ *we have a type III separatrix configuration as above (Figures 4 and 8).* ■

We consider the Catalan trisectrix $y = \pm x\sqrt{1-x}$*, rescaled in x and y, rotated by* 60° *and translated such that its left vertex will be in the saddle. It will be parametrized as* $(x(t), y(t))$*.* $a = 0.09,\ b = 0.105,\ c = 0.3,\ d = 1,\ B = 0.2.$ $x_1(t) = \left(\frac{a}{b}\right)\left(\sin\left(\frac{t}{2}\right)\right)^2$*,* $y_1(t) = \frac{a\sqrt{a}}{b}\cos\left(\frac{t}{2}\right)\left(\sin\left(\frac{t}{2}\right)\right)^2$*.*

$$x(t) = d\cdot\left(\tfrac{1}{2}x_1(t) + \tfrac{\sqrt{3}}{2}y_1(t) - c\right) \qquad y(t) = d\cdot\left(-\frac{\sqrt{3}}{2}x_1(t) + \tfrac{1}{2}y_1(t) + \tfrac{5}{3}c\right).$$

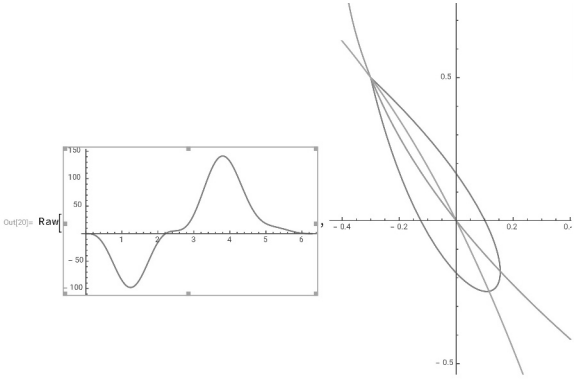

Figure 9. The the graphs of $F(t) = P(Z(t))y'(t) - Q(Z(t))x'(t)$ and of the Catalan trisectrix $(x(t), y(t))$

It has the following property, as in can be seen from Figure 9: For $t \in (0, t_0)$ *the field lines enter inside the curve. For* $t = t_0$ *it has a contact with the flow. For* $t \in (t_0, 2\pi)$ *the field lines exit the curve interior.* $F(t)$ *is a polynomial in* $\sin(t/2)$ *and* $\cos(t/2)$ *of degree 9. For* $\sin(\frac{t}{2}) = \frac{2z}{1+z^2}$ *and* $\cos(\frac{t}{2}) = \frac{1-z^2}{1+z^2}$ *the sign is given by a degree 18 real polynomial in* z*.*

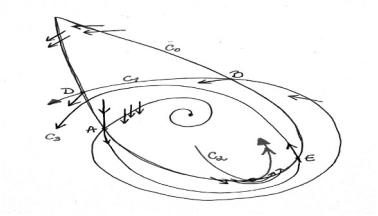

Figure 10. The Catalan trisectrix; the solution curve C_2 contains the only contact point between the vector field and the Catalan curve

We have a separatrix configuration of Figure 4, type III. Suppose by contradiction that all trajectories go from the origin to the second anti-saddle, or towards the saddle in the case of the stable manifold. We take an orbit, spiral out from the origin. We deform it using Gasull's corollary mentioned at the beginning of the Section 3.1 in such a way the field lines go inside it as in Figure 10. C_1 *is this transversal curve to the flow.*

The first 3 intersection points between C_0 *-the Catalan curve and* C_1 *are A, B and D.* C_3*= the solution curve for the flow containing A. We also have the solution curve*

C_2, which contains the contact point between C_0 and the flow. As we can see in Figure 10 above, the only way to have a "convex spiral out" pattern, with a positive displacement map is for C_2 to contain the point A. But the position of $A \in C_0 \cap C_1$ can be modified. C_2 is a fixed solution curve which passes through the only contact point between C_0 and the flow. In conclusion, we do not have the situation in which all trajectories spiral out from the origin, so we have at least two limit cycles, a stable one surrounded by a bigger unstable limit cycle, in a Figure 4, Type III configuration. ■

The trigonometric expansion of $F(t)$, the function which measures the transversality of the Catalan trisectrix with respect to the flow is:
0.00117697 Sin[t/2]-0.00209297 Sin[t]-0.00152813 Sin[(3 t)/2]+0.0005613 Sin[2 t]-
-0.000127706 Sin[(5 t)/2]-0.000254774 Sin[3 t]+0.00063798 Sin[(7 t)/2]+
+0.000433673 Sin[4 t]-0.0000466552 Sin[(9 t)/2]. $t \in [0; 2\pi]$.

Remark: According to [12] and [9], the possible local bifurcation for a bounded quadratic system are: saddle-node bifurcations, Hopf bifurcations of codim. 1 and 2, Bogdanov-Takens bifurcations, saddle-saddle bifurcations, homoclinic-loop and multiplicity–two limit cycle bifurcations. For $B = 0.2$ and $p = -0.7$, all field lines go out from the Catalan trisectrix for any d between 0.95 and 1.
Figure 11 is the graph of F(t). If we suppose by contradiction that we had Figure 5, Type I configuration for the stable and the unstable manifolds, then the stable limit cycle for $p = 0$ has to disappear at $p = -0.7$. A homoclinic loop bifurcation (which has to be located in the $Tr(saddle) > 0$ *zone*) or a multiplicity 2 – limit cycle bifurcation curve automatically involves another unstable limit cycle, containing a stable one inside it. In this way we justify Figure 4, Type III configuration –using again the Catalan curve, without mentioning the saddle-saddle bifurcation (Lemma 6.3).

7 Discussion

A challenge is to vizualize the four limit cycles of these systems "on the same screen". Future research directions could be the global bifurcations and the number of limit cycles around the second anti-saddle. Previous studies ([19]) and working hypotheses (the use of computers) were against the conclusion that there exist quadratic systems with four

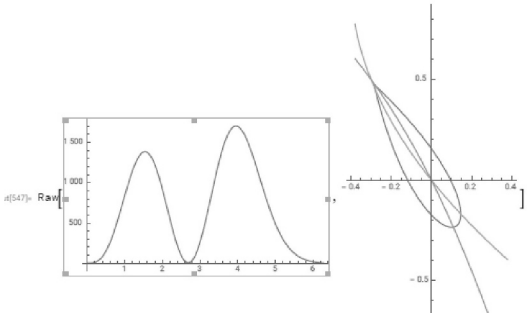

Figure 11. The graphs of $F(t) = P(Z(t))y'(t) - Q(Z(t))x'(t) > 0$ and of the Catalan curve $(x(t), y(t))$, for $B = 0.2; p = -0.7; d = 0.95; a = 0.09; b = 0.105; c = 0.3$

limit cycles around a singularity. Dynamical systems were also used in self-assembly [29] to model probabilities or species concentrations.

7.1 Positive polynomials, signal processing and (a super-version of) the 17^{th} Hilbert's problem

Hilbert's 17^{th} problem, posed at ICM Paris(1900), ask if a non-negative polynomial of n variables can be written as a sum of squares of rational functions. The problem was solved by Artin (1927). Hilbert's problem was generalized to polynomials defined on intervals and to positive trigonometric polynomials applied in optimization, engineering, in signal processing [30], [31], [32]. The trigonometric polynomials which have exactly one root on a given interval - as the trigonometric polynomials $F(t)$ generated by the Catalan trisectrix - are much complicated and their theoretical and numerical study could be relevant for our instance of planar Hilbert's 16^{th} problem.

8 Materials and Methods

The theoretical results about dynamical systems are essential on proving the existence of 4 limit cycles around the origin for $B = 0.5 * \left(1.7 - \sqrt{1.29}\right) + \epsilon_1$ and $p = -\epsilon_2$ and ϵ_{1or2} strictly positive and very small. Theoretically, we do not know how small ϵ_i should be.
Conjecture: For $B = 0.5 * \left(1.7 - \sqrt{1.29}\right) + 0.003$ and $p = -0.0001$ the dynamical system (3) has four limit cycles around the origin.

For these values, the Mathematica computations show that the equation (7) has two

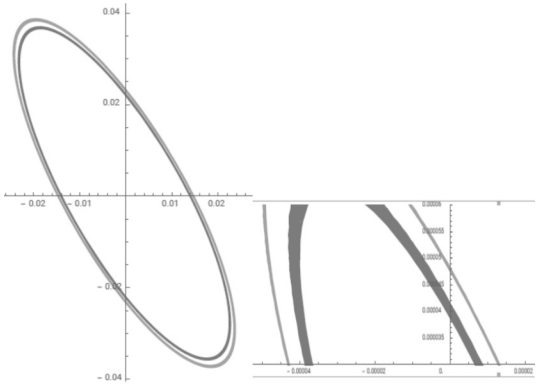

Figure 12. The unstable limit cycle intersects the Oy-axis between 0.022 and 0.023; the stable limit cycle intersects the Oy-axis between 0.000038 and 0.000048 (for B=0.2 and p=0, initial conditions of the four orbits above: x=0 and the mentioned values for y)

strictly positive roots. A general statement about the analytical coefficients of equation (7) symbolically computed in Mathematica is required. For

$$\begin{cases} \dot{x} = -x - 0,8y + 0,4y^2 \\ \dot{y} = 2x + y - xy - 0.2y^2. \end{cases} \tag{9}$$

the behaviour of the Poincare (or return, or cross-section) map – $P(z)$ compared to z–for the following initial values (starting point) are easy to be visualised on Mathematica Cloud (or Mathematica and Matlab): x=0.0 and $y \in [0.1; 0.02; 0.022; 0.023; 0.001; 0.05; 0.000038; 0.000048]$. The transversal curve used in Section 5 (Figure 10) could be replaced by any spiral-out trajectory. We esentially use the Catalan (or L'Hospital) trisectrix to prove the above mentioned results, in a way which can be algoritmically checked using the provided parameters.

9 Conclusions

The systems (3) came from a natural inverse problem: to find, for random data (stochastic simulations using NFsim which generated quasi-cycles), biologically -relevant chemical reaction networks. For $p = 0$ and $B = 0.6$ we found a dynamical system from the family (3) above, such that there is a CRN with its prescribed dynamics of concentrations (Section 6).

The systems (3) are counterexamples to a Perko's conjecture [12] (it was conjectured

that a bounded planar quadratic system has at most 2 limit cycles). In the recent [33], 14 types of planar 2-polynomial systems have unknown global bifurcation structure- some of them can be found among our systems. The behavior of the L'Hospital cubic with respect to the system and its way to provide a proof of the existence of 2 new (global, in any case non-local) limit cycles can be generalized to other coefficients, if all ingredients of the proof above are satisfied: we mention the positions of the weak focus of order 2 and of the intersections between the saddle-saddle connection curve and zero-divergence curve with the 1-dim Hopf bifurcation line in the bifurcation diagram. Inequalities involve roots of polynomials of degree at least 5. The appeareance of the *bounded* planar quadratic systems is explained by their biochemical origins.

10 Appendix. The second anti-saddle

The second anti-saddle is relevant for the dynamics of x and y concentrations for:

$Y() \to Y() + Y()$ (kinetic rate $k_1 = 0.2$) ;$X() + Y() \to X() + P()(k_2 = \frac{2}{3})$; $Y() + Y() \to X() + Y()$ $(k_3 = \frac{6}{10})$; $S() + X() \to Y() + Y()$ $(k_4 = \frac{1}{3000000})$; $X() \to P()$ $(k_5 = \frac{2}{3})$

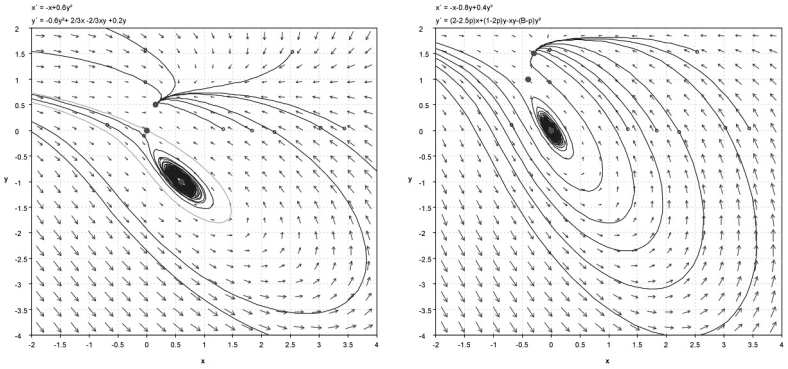

Figure 13. Dynamics of species concentrations become the dynamical system (3) for $B = 0.6$ and $p = 0.0$ if the lower anti-saddle is translated to the origin.

The first quadrant is invariant for the flow of the system $\frac{dx}{dt} = -x + 0.6y^2$; $\frac{dy}{dt} = -0.6y^2 + \frac{2}{3}x - \frac{2}{3}xy + 0.2y$. The second anti-saddle is the only stable node. If we translate the lower anti-saddle to the origin, the phase space become the phase space of the dynamical system (3) for $B = 0.6$ and p=0.0. There are no limit cycles around this stability node for the system. To study the second anti-saddle, we have to go back to the bifurcation

diagram of the family (3).

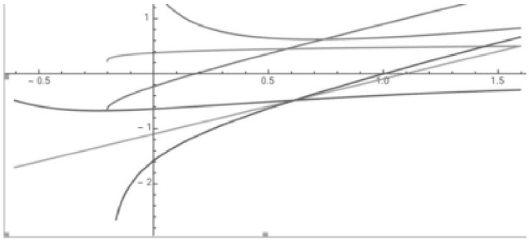

{{x → 0.595507 − 0.591005 i}, {x → 0.595507 + 0.591005 i}}

{{x → 2.12759}}

{{x → −1.98987}, {x → −0.201018}, {x → 1.82574}}

{{x → 0.740172}}

{{x → 0.613248}}

{{x → 0.611019}}

Figure 14. The line is the 1-dim Hopf curve for the origin. There are two very close intersections between this line and the weak focus of order 2 curve for the origin, and the zero-divergence curve.A system with an unstable homoclinic loop can appear only below the second curve (upside-down parabolic shape), where the divergence at the saddle is > 0. The upper parabolic curve is the 1-dim Hopf curve for the second anti-saddle. The last numbers are the x-coordinates of the intersections among these 6 curves (the weak focus of order 2 curve for the second anti-saddle (in our case, there is no focus of order 2 for the second anti-saddle and the solutions are complex);the saddle-saddle connection curve,).

The oX-axis = the α coefficient $=\sqrt{1.6} - \frac{B}{\sqrt{0.4}}$. The oY-axis = $c = \frac{p-B}{\sqrt{0.4}}$. $\beta = -\sqrt{1.6}$ and $\gamma = \sqrt{0.6}$.

The trace of the Jacobian matrix evaluated at the second anti-saddle (x_2, y_2) vanishes if:

$c(\alpha+S) = 1+\alpha(\alpha+\beta+S)/2$, where $S = \sqrt{(\alpha-\beta)^2 - 4\gamma^2}$ (Theorem 5, Chapter 4.14, [9]). In this case the systems (3) have (α,c)-coeficients on the highest convex curve from Figure 14.

The second anti-saddle (x_2, y_2) is a weak focus of order 2 if $2ac + b = \sqrt{(b^2 - 4ad}$, where $d = \beta - \alpha - 3S$, $a = 4S - 2\beta$ and $b = 2 + (\alpha + \beta - S)(\beta - 2S)$.(Theorem 5, Chapter 4.14, [9]).

In our case we do not have a weak focus of order 2. The solutions are the first complex numbers from Figure 14.

The second anti-saddle is unstable for the coefficients (α,c) above the highest convex curve from Figure 14. It is stable below this curve (in particular for B=0.6 and p=0.0). Transversal passing of this curve by increasing p will generate a stable limit cycle from a supercritical Hopf bifurcation around a second anti-saddle.

To find non-local limit cycles around the second anti-saddle as we proceeded for the origin, we need systems which cannot represent chemical reaction networks, and 2-parameter families which satisfy this condition for all of its members. In this way, in the vicinity of the intersection between 1-dimensional Hopf bifurcation curves for the origin and for the second anti-saddle, we could find planar quadratic dynamical systems with more than 4 limit cycles.

Acknowledgments: This research was funded by [the Romanian National Authority for Scientific Research project MoDASyS, co-funded by the European Fund of Regional Development] grant number [POC P-37-257].

References

[1] E. Czeizler, P. Orponen, Yield optimization strategies for (DNA) staged tile assembly systems, in: A. H. Dediu, C. Martín–Vide, B. Truthe, M. A. Vega–Rodríguez (Eds.), *Theory and Practice of Natural Computing Second International Conference*, Springer, Berlin, 2013, pp. 31–44.

[2] E. Demaine, S. Eisenstat, M. Ishaque, A. Winslow, One–dimensional staged self–assembly, *Nat. Comput.* **12** (2013) 247–258.

[3] A. Amarioarei, G. Barad, E. Czeizler, E. Czeizler, A. M. Dobre, A. Paun, M. Paun, One dimensional DNA tiles self assembly model simulation, *Int. J. Unconv. Comput.* **13** (2018) 399–415.

[4] J. R. Faeder, M. L. Blinov, W. S. Hlavacek, Rule–based modeling of biochemical networks with BioNetGen, *Meth. Mol. Biol.* **500** (2009) 1–55.

[5] L. H. Kauffman, Map coloring and the vector cross product, *J. Comb. Theory B* **48** (1990) 145–154.

[6] G. Gruenert, B. Ibrahim, T. Lenser, T. Hinze, P. Dittrich, Rule–based spatial modeling with diffusing, geometrically constrained molecules, *BMC Bioinf.* **11** (2010) #307.

[7] G. A. Leonov, N. V. Kuznetsov, Hidden attractors in dynamical systems. From hidden oscillations in Hilbert–Kolmogorov, Aizerman, and Kalman problems to hidden chaotic attractor in Chua circuits, *Int. J. Bifurcat. Chaos* **23** (2013) #1330002.

[8] J. Llibre, Z. F. Zhang, Weak focus, limit cycles, and bifurcations for bounded quadratic systems, *J. Diff. Eqs.* **115** (1995) 193–223.

[9] L. M. Perko, *Differential Equations and Dynamical Systems*, Springer, New York, 2013.

[10] C. Rousseau, Example of a quadratic system with two cycles appearing in a homoclinic loop bifurcation, *J. Diff. Eqs.* **66** (1987) 140–150.

[11] P. Yu, R. Corless, Symbolic computation of limit cycles associated with Hilbert's 16^{th} problem, *Commun. Nonlin. Sci.* **14** (2009) 4041–4056.

[12] F. Dumortier, C. Herssens, L. M. Perko, Local bifurcations and a survey of bounded quadratic systems, *J. Diff. Eqs.* **165** (2000) 430–467.

[13] R. J. Dickson, L. M. Perko, Bounded quadratic systems in the plane, *J. Diff. Eqs.* **7** (1970) 251–273.

[14] P. Yu, W. Lin, Complex dynamics in biological systems arising from multiple limit cycle bifurcation, *J. Biol. Dyn.* **10** (2016) 263–285.

[15] Y. Ilyashenko, Towards the general theory of global planar bifurcations, in: B. Toni (Ed.), *Mathematical Sciences with Multidisciplinary Applications*, Springer, Cham, 2016, pp. 269–299.

[16] S. Songling, A concrete example of the existence of four limit cycles for plane quadratic systems, *Sci. Sinica* **23** (1980) 153–158.

[17] M. Wang, L. Chen, Relative position and number of limit cycles of a quadratic differential system, *Acta Math. Sinica* **22** (1979) 751–758.

[18] C. Rousseau, D. Schlomiuk, Generalized Hopf bifurcations and applications to planar quadratic systems, *Ann. Pol. Math.* **49** (1988) 1–16.

[19] J. Tian, A survey of Hilbert's sixteenth problem, in: B. D. Sleeman, R. J. Jarvis (Eds.), *Ordinary and Partial Differential Equations*, Longman, Harlow, 1988, pp. 178–203.

[20] G. Armengol, H. Giacomini, G. Maite, Proving the existence of numerically detected planar limit cycles, (2016) arXiv: 1602.00113 .

[21] H. Giacomini, M. Grau, Transversal conics and the existence of limit cycles, *J. Math. Anal. Appl.* **428** (2015) 563–586.

[22] A. Gasull, H. Giacomini, M. Grau, Effective construction of Poincaré–Bendixson regions, *J. Appl. Anal. Comput.* **7** (2017) 1549–1569.

[23] L. M. Perko, Rotated vector fields, *J. Diff. Eqs.* **103** (1993) 127–145.

[24] N. V. Kuznetsov, *Stability and oscillation of dynamical systems: theory and applications*, Ph.D. Thesis, Univ. Jyväskylä, 2008.

[25] J. C. Artés, J. Llibre, D. Schlomiuk, N. Vulpe, Geometric configurations of singularities for quadratic differential systems with three distinct real simple finite singularities, *J. Fix Point Theory A* **14** (2013) 555–618.

[26] L. M. Perko, Homoclinic loop and multiple limit cycle bifurcation surfaces, *Trans. Am. Math. Soc.* **344** (1994) 101–130.

[27] Wolfram Research, Inc., Mathematica, Version 11.2, Champaign, IL (2018); Wolfram Research, Inc. (www.wolfram.com), Wolfram Development Platform, Champaign, IL (2018); Mathematica Online, Champaign, 2018.

[28] J. C. Polking, D. Arnold, *Ordinary Differential Equations Using MATLAB*, Pearson, Prentice Hall, 2004.

[29] S. Miyashita, M. Goldi, R. Pfeifer, How reverse reactions influence the yield of self–assembly robots, *Int. J. Robot Res.* **30** (2011) 627–641.

[30] T. Roh, L. Vandenberghe, Discrete transforms, semidefinite programming, and sum–of–squares representations of nonnegative polynomials, *SIAM J. Opt.* **16** (2006) 939–964.

[31] K. Schmudgen, Around Hilbert's 17*th* problem. Optimization stories, *Doc. Math.* (2012) 433–438.

[32] B. Dumitrescu, *Positive Trigonometric Polynomials and Signal Processing Applications*, Springer, Cham, 2017.

[33] J. Llibre, X.Zhang, The non-existence, existence and uniqueness of limit cycles for quadratic polynomial differential systems, *Proc. Roy. Soc. Edinburgh A* (2017) 1–14.

[34] D. Dudkowski, S. Jafari, T. Kapitaniak, N. V. Kuznetsov, G. A. Leonov, A. Prasad, Hidden attractors in dynamical systems, *Phys. Rep.* **637** (2016) 1–50.